The Journal of Immunology

The Phagocyte Oxidase Controls Tolerance to *Mycobacterium tuberculosis* Infection

Andrew J. Olive, Clare M. Smith, Michael C. Kiritsy and Christopher M. Sassetti

J Immunol 2018; 201:1705-1716; Prepublished online 30 July 2018;
doi: 10.4049/jimmunol.1800202
http://www.jimmunol.org/content/201/6/1705

The Journal of Immunology is published twice each month by
The American Association of Immunologists, Inc.,
1451 Rockville Pike, Suite 650, Rockville, MD 20852

Print ISSN: 0022-1767 Online ISSN: 1550-6606.

The Phagocyte Oxidase Controls Tolerance to *Mycobacterium tuberculosis* Infection

Andrew J. Olive,[1] Clare M. Smith, Michael C. Kiritsy, and Christopher M. Sassetti

Protection from infectious disease relies on two distinct strategies: antimicrobial resistance directly inhibits pathogen growth, whereas infection tolerance protects from the negative impact of infection on host health. A single immune mediator can differentially contribute to these strategies in distinct contexts, confounding our understanding of protection to different pathogens. For example, the NADPH-dependent phagocyte oxidase (Phox) complex produces antimicrobial superoxide and protects from tuberculosis (TB) in humans. However, Phox-deficient mice display no sustained resistance defects to *Mycobacterium tuberculosis*, suggesting a more complicated role for NADPH Phox complex than strictly controlling bacterial growth. We examined the mechanisms by which Phox contributes to protection from TB and found that mice lacking the Cybb subunit of Phox suffered from a specific defect in tolerance, which was caused by unregulated Caspase-1 activation, IL-1β production, and neutrophil influx into the lung. These studies imply that a defect in tolerance alone is sufficient to compromise immunity to *M. tuberculosis* and highlight a central role for Phox and Caspase-1 in regulating TB disease progression. ***The Journal of Immunology*****, 2018, 201: 1705–1716.**

Protective defense to infectious disease involves functionally overlapping responses that can be divided into two fundamentally different categories (1, 2). Infection resistance refers to functions that directly target the infecting pathogen to prevent its growth and dissemination. Resistance pathways act by a variety of mechanisms, including disrupting the bacterial niche, serving as metabolic poisons, and sequestering critical nutrients (3–5). In addition, the extent of disease is also influenced by tolerance strategies that enhance host survival but do not directly impact pathogen growth (6–8). Tolerance pathways control a broad range of functions that protect the infected tissues from the direct cytotoxic properties of the pathogen as well as inflammation-mediated immunopathologic condition and enhance the overall health of the host in the face of an ongoing infection. Although it is well appreciated that both resistance and tolerance mechanisms are required to limit disease, the relative importance of these pathways vary for different infections (1). Furthermore, because individual immune effectors can promote both tolerance and resistance, the specific role for each mediator can change in different contexts (1, 6, 9–11). In the context of chronic infections, where resistance mechanisms are insufficient and the pathogen persists in the tissue, tolerance is likely to play a particularly important role (11).

Like many other chronic infections, the outcome of an encounter with *Mycobacterium tuberculosis* varies dramatically between individuals (12). Only 5–10% of those that are infected with this pathogen progress to active tuberculosis (TB), and disease progression is influenced by a wide variety of genetic and environmental factors that modulate either tolerance or resistance (13–15). For example, observations from humans and mice indicate that several specific changes in T cell function may contribute to a failure of resistance and disease progression caused by loss of antimicrobial resistance (16–18). In addition, studies in animal models indicate that a failure of host tolerance, which is necessary to preserve lung function or granuloma structure, influences the extent of disease (19, 20). Although these studies suggest that variation in overall tolerance may be an important determinant TB risk, the specific tolerance mechanisms that influence disease progression in natural populations remain ill defined. Furthermore, because most immune mediators are pleiotropic and affect both tolerance and resistance, it remains unclear if a specific failure of tolerance alone can promote TB disease progression.

During many bacterial infections, the production of reactive oxygen species (ROS) by the NADPH phagocyte oxidase (Phox) is involved in protecting the host from disease (21). Phox is a multiprotein complex, including the subunits Cybb (gp91) and Ncf1 (p47) that assemble in activated immune cells to produce superoxide radicals by transferring electrons from NADPH to molecular oxygen (22). Humans with deleterious mutations in the Phox complex develop a clinical syndrome known as chronic granulomatous disease (CGD). Leukocytes from patients with CGD are unable to kill a number of bacterial pathogens, such as *Staphylococcus aureus* and *Serratia marcescens*, and this defect is associated with the susceptibility to infection with these organisms (23). Because ROS contributes to the microbicidal activity of phagocytes, previous studies in *M. tuberculosis*–infected mice focused on the role of Phox in antimicrobial resistance. Several such studies found that mice deficient in Phox show no

University of Massachusetts Medical School, Worcester, MA 01605

[1]Current address: Michigan State University, East Lansing, MI.

ORCIDs: 0000-0003-3441-3113 (A.J.O.); 0000-0003-2601-0955 (C.M. Smith); 0000-0001-8364-8088 (M.C.K.).

Received for publication February 12, 2018. Accepted for publication July 11, 2018.

This work was supported by the Arnold and Mabel Beckman Postdoctoral Fellowship (to A.J.O.), the Charles King Trust Postdoctoral Fellowship (to C.M. Smith), and National Institutes of Health Grant AI132130 (to C.M. Sassetti).

A.J.O. and C.M. Sassetti conceived of and designed the experiments. A.J.O., C.M. Smith, and M.C.K. performed the experiments and analyzed the data. A.J.O. and C.M. Sasssetti wrote the initial manuscript. All authors edited the manuscript.

Address correspondence and reprint requests to Dr. Christopher M. Sassetti, University of Massachusetts, 368 Plantation Street, ASC8-2051, Worcester, MA 01605. E-mail address: Christopher.Sassetti@umassmed.edu

The online version of this article contains supplemental material.

Abbreviations used in this article: BCG, bacillus Calmette–Guérin; BMDC, bone marrow–derived dendritic cell; BMDM, bone marrow–derived macrophage; CGD, chronic granulomatous disease; Phox, phagocyte oxidase; ROS, reactive oxygen species; TB, tuberculosis.

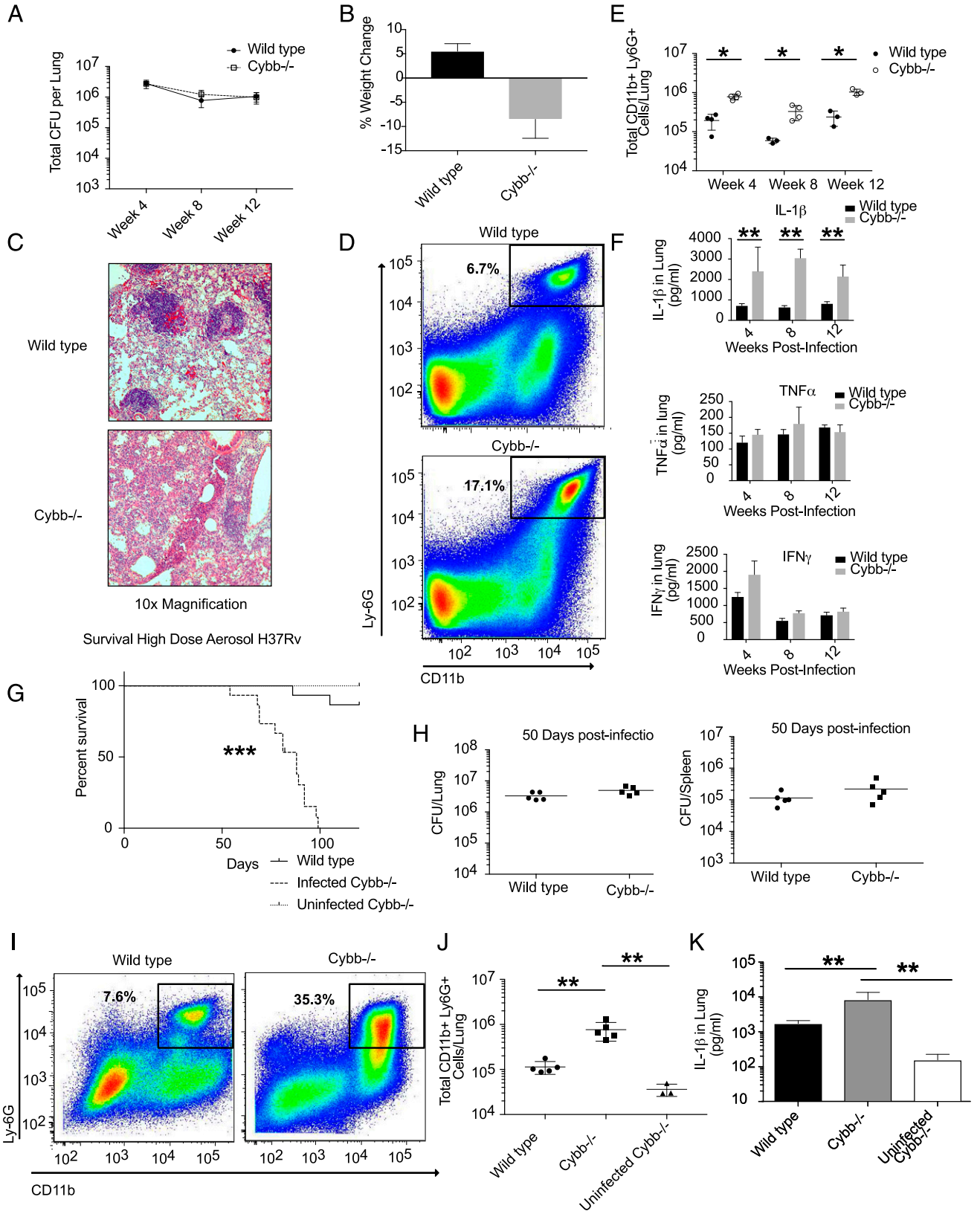

FIGURE 1. Anti-inflammatory activity of Cybb protects mice from TB disease. (**A**) Following low-dose aerosol infection (day 0 of ~50–100 CFU), total bacterial burden (expressed in CFU, mean ± SD) was determined in the lungs of wild type or *Cybb*$^{-/-}$ mice at the indicated time points with four to five mice per group. (**B**) Percentage weight loss (mean change ± SD) from day 0 to day 100 was determined for wild type and *Cybb*$^{-/-}$ mice. Representative of two experiments with three to five mice per group. (**C**) Immunohistochemical staining for H&E is shown for representative lung sections from wild type and *Cybb*$^{-/-}$ mice at 8 wk postinfection at original magnification ×20. (**D**) Representative flow cytometry plot showing increased Ly6G^{+} CD11b^{+} neutrophil recruitment to the lungs of *Cybb*$^{-/-}$ mice 4 wk postinfection (gated on live/singlets/CD45^{+}). (**E**) Quantification of neutrophil recruitment to the lungs at the indicated time points postinfection for wild type and *Cybb*$^{-/-}$ mice is shown as absolute number of Ly6G^{+} CD11b^{+} cells per lung (mean ± SD). Representative of four experiments with three to five mice per group. *$p < 0.05$, unpaired two-tailed *t* test. (**F**) Lung homogenates *(Figure legend continues)*

long-term differences in *M. tuberculosis* bacterial levels compared with wild type animals (24–26). Cooper et al. (24) observed a transient increase in bacterial numbers between 15 and 30 d postinfection of Ncf1$^{-/-}$ mice, but this difference was not sustained. Two subsequent studies found that no difference in *M. tuberculosis* burden could be attributed to Cybb deficiency (25, 26). The lack of an obvious antimicrobial role for Phox during *M. tuberculosis* infection is likely due to the expression of mycobacterial ROS defenses. These defenses include the catalase/peroxidase KatG, which detoxifies ROS directly, and the MRC complex that detoxifies a variety of radicals (26–29). Together, these bacterial defense mechanisms may allow *M. tuberculosis* to withstand the oxidative killing mechanisms (30). In contrast to the apparent dispensability of Phox in short-term mouse infections with *M. tuberculosis*, human mutations in the *Cybb* gene are strongly associated with susceptibility to mycobacterial diseases, including TB (31–35). Mutations that specifically reduce Cybb activity in macrophages produce a similar clinical presentation, highlighting the importance of the macrophage-derived ROS in protection (31). Taken together, although Phox is clearly important for controlling mycobacterial diseases, including TB, the absence of long-term resistance defects in *M. tuberculosis*–infected mice suggests that the Phox may play a more complex role than simply limiting bacterial replication.

In this study, we examined the mechanisms of Phox-mediated protection in the context of *M. tuberculosis* infection. We found that loss of the Phox subunit Cybb does not alter the growth or survival of *M. tuberculosis* during infection. Instead, *Cybb*$^{-/-}$ animals suffered from a hyperinflammatory disease caused by increased activation of the NLRP3-dependent Caspase-1 inflammasome and IL-1–dependent neutrophil accumulation in the lung. Thus, the protective effect of Phox can be solely attributed to increased tolerance to *M. tuberculosis* infection instead of a direct antimicrobial effect. These studies provide a mechanism to explain the association between Phox expression and TB disease in natural populations and implicate control of Caspase-1 activation as an important regulator of infection tolerance.

Materials and Methods

Mice

C57BL/6J (stock no. 000664), *Cybb*$^{-/-}$ (B6.129S-Cybb^{tm1Din}/J stock no. 002365), Nos2$^{-/-}$ (B6.129P2-Nos2^{tm1Lau}/j, stock no. 002609), and B6.SJL-*Ptprc*^{a} *Pepc*^{b} carrying the pan leukocyte marker CD45.1 (stock no. 002014) were purchased from The Jackson Laboratory. Mice were housed under specific pathogen-free conditions and in accordance with the University of Massachusetts Medical School Institutional Animal Care and Use Committee guidelines. All animals used for experiments were 6–12-wk except mixed chimeras that were infected at 16-wk following 8 wk of reconstitution.

Mouse infection

Wild type *M. tuberculosis* strain H37Rv was used for all studies unless indicated. This strain was confirmed to be PDIM-positive. Prior to infection, bacteria were cultured in 7H9 medium containing 10% oleic albumin dextrose catalase growth supplement enrichment (Becton Dickinson) and 0.05% Tween-80. H37Rv expressing sfYFP has been previously described, and the episomal plasmid was maintained with selection in hygromycin B (50 μg/ml) added to the media (10). For low- and high-dose aerosol infections, bacteria were resuspended in PBS containing Tween-80. Prior to infection, bacteria were sonicated and then delivered via the respiratory route using an aerosol generation device (Glas-Col). Infections of mice with the streptomycin-dependent strain of *M. tuberculosis* (18b) have been previously described (36). In short, mice were infected via intratracheal infection and treated daily with 2 mg of streptomycin for 2 wk. For anti–IL-1R treatment, mice were injected with 200 μg of anti–IL-1R Ab or Isotype control (Bio X Cell) every other day starting at day 14. Both male and female mice were used throughout the study, and no significant differences in phenotypes were observed between sexes.

Immunohistochemistry

Lungs from indicated mice were inflated with 10% buffered formalin and fixed for at least 24 h, then embedded in paraffin. Five-micrometer–thick sections were stained with H&E. All staining was done by the Diabetes and Endocrinology Research Center Morphology Core at the University of Massachusetts Medical School.

Flow cytometry

Lung tissue was harvested in DMEM containing FBS and placed in C Tubes (Miltenyi Biotec). Collagenase Type IV/DNase I was added, and tissues were dissociated for 10 s on a gentleMACS system (Miltenyi Biotec). Tissues were incubated for 30 min at 37°C with oscillations and then dissociated for an additional 30 s on a gentleMACS. Lung homogenates were passaged through a 70-μm filter or saved for subsequent analysis. Cell suspensions were washed in DMEM, passed through a 40-μm filter, and aliquoted into 96-well plates for flow cytometry staining. Nonspecific Ab binding was first blocked using Fc Block. Cells were then stained with anti–Ly-6G Pacific Blue, anti-CD4 Pacific Blue, anti-CD11b PE, anti-CD11c APC, anti–Ly-6C APC-Cy7, anti-CD45.2 PercP Cy5.5, anti-CD3 FITC, anti-CD8 APC-Cy7, and anti-B220 PE-Cy7 (BioLegend). Live cells were identified using LIVE/DEAD Fixable Aqua (Life Technologies). For infections with fluorescent H37Rv, lung tissue was prepared as above, but no Abs were used in the FITC channel. All of these experiments contained a nonfluorescent H37Rv infection control to identify infected cells. Cells were stained for 30 min at room temperature and fixed in 1% paraformaldehyde for 60 min. All flow cytometry was run on a MACSQuant Analyzer 10 (Miltenyi Biotec) and was analyzed using FlowJo V9 (Treestar).

Macrophage and dendritic cell generation

To generate bone marrow–derived macrophages (BMDMs), marrow was isolated from femurs and tibia of age- and sex-matched mice. Cells were then incubated in DMEM (Sigma-Aldrich) containing 10% FBS and 20% L929 supernatant. Three days later, media were exchanged with fresh media, and 7 d postisolation, cells were lifted with PBS-EDTA and seeded in DMEM containing 10% FBS for experiments.

To generate bone marrow–derived dendritic cells (BMDCs), marrow was isolated from femurs and tibia of age- and sex-matched mice. Cells were then incubated in IMDM media (Life Technologies) containing 10% FBS, L-Glutamine, 2 μM of 2-ME, and 10% B16–GM-CSF supernatant (37). BMDCs were then purified on day 6 using Miltenyi Biotec LS Columns first using negative selection for F480 followed by CD11c positive selection. Cells were then plated and infected the following day.

Macrophage and dendritic cell infection

M. tuberculosis or *M. bovis* bacillus Calmette–Guérin (BCG) were cultured in 7H9 medium containing 10% oleic albumin dextrose catalase growth

from wild type or *Cybb*$^{-/-}$ mice infected for the indicated time were probed for the cytokines IL-1β, IFN-γ, and TNF-α by ELISA (mean ± SD). Results shown in (A)–(D) are representative of three independent experiments with three to five mice per group. $^{**}p < 0.01$, unpaired two-tailed *t* test. (**G**) Survival of infected wild type and *Cybb*$^{-/-}$ and uninfected *Cybb*$^{-/-}$ mice was determined following high-dose infection. Data are representative of two independent experiments with 14–15 mice per group. $^{***}p < 0.001$, Mantel–Cox text. (**H**) Fifty days following high-dose aerosol infection (day 0 of 5000–7500 CFU), total bacterial burden (expressed in CFU, mean ± SD) was determined in the lungs and spleen of wild type or *Cybb*$^{-/-}$ mice. Data are representative of two experiments with four to five mice per group. (**I**) Representative flow cytometry plot showing increased Ly6G^{+} CD11b^{+} neutrophil recruitment to the lungs of *Cybb*$^{-/-}$ mice 50 d postinfection (gated on live/singlets/CD45^{+}). (**J**) Quantification of the absolute number of neutrophils recruited to the lungs 50 d following high-dose infection for wild type and *Cybb*$^{-/-}$ mice is shown (mean ± SD). Representative of two experiments with five mice per group. $^{**}p < 0.01$, one-way ANOVA with Tukey correction. (**K**) Lung homogenates from uninfected *Cybb*$^{-/-}$ mice and wild type or *Cybb*$^{-/-}$ mice infected for 50 d following high-dose aerosol were probed for IL-1β by ELISA (mean ± SD). $^{**}p < 0.01$, unpaired two-tailed *t* test. Results shown in (G)–(J) are representative of two independent experiments with five mice per group. $^{**}p < 0.01$, unpaired two-tailed *t* test.

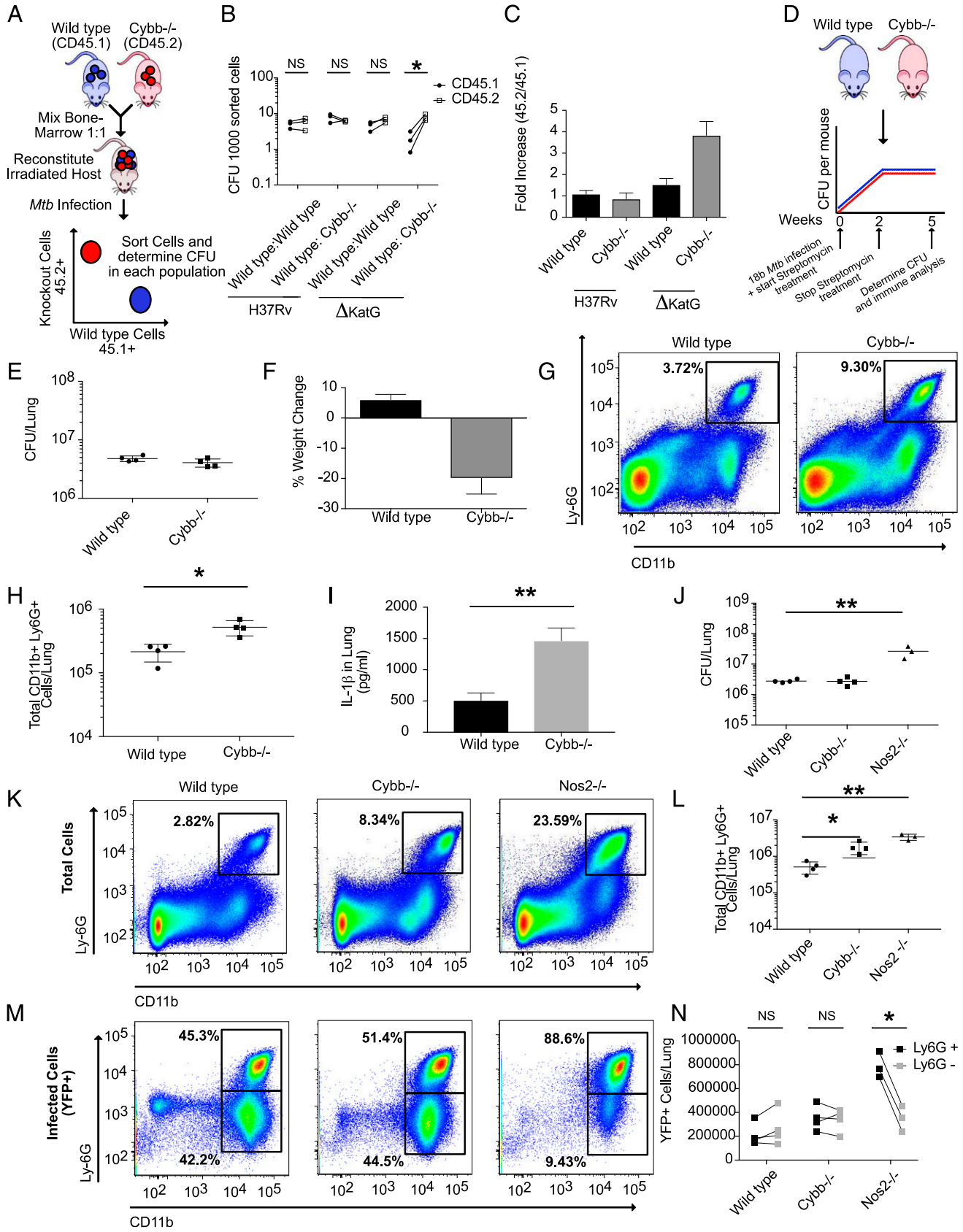

FIGURE 2. The primary protective role of Cybb is anti-inflammatory. (**A**) Schematic for the generation of mixed bone marrow chimeras. Mixed bone marrow chimeras were infected by low-dose aerosol with either H37Rv or ΔKatG mutant. Five weeks postinfection, CFU levels were determined in purified hematopoietic cells of indicated genotypes. (**B**) Shown are the normalized CFU per sorted cells in each population from each mouse. *$p < 0.05$, unpaired two-tailed t test. (**C**) The fold increase of bacterial levels in CD45.2$^+$ cells (experimental) compared with CD45.1$^+$ cells (wild type control) (mean ± SD). The results in (B) and (C) are representative of three independent experiments with three to four mice per group. (**D**) Schematic for streptomycin-dependent infection. Wild type and *Cybb*$^{-/-}$ mice were infected intratracheally with *M. tuberculosis* strain 18b and treated for 2 wk daily *(Figure legend continues)*

supplement enrichment (Becton Dickinson) and 0.05% Tween 80. Before infection, cultures were washed in PBS-Tween, resuspended in DMEM containing 10% FBS, and passed through a 5-μm filter to ensure single cells. Multiplicity of infection was determined by OD with an OD of one being equivalent to 3×10^8 bacteria/ml. Bacteria were added to macrophages for 4 h, then cells were washed with PBS, and fresh media were added. At the indicated time points, supernatants were harvested for cytokine analysis, and the cells were processed for further analysis. Cell death was assessed using CellTiter-Glo Luminescent Cell Viability Assay (Promega) following manufacturer's instructions. For inhibitor treatments, cells were treated with the indicated concentrations of IFN-γ (PeproTech), MCC950 (Adipogen), VX-765 (InvivoGen), or vehicle control overnight prior to infection and maintained in the media throughout the experiment.

Mixed bone marrow chimera generation and cell sorting

Mixed bone marrow chimera experiments were done essentially as previously described (10). Wild type CD45.1$^+$ mice were lethally irradiated with two doses of 600 rad. The following day, bone marrow from CD45.1$^+$ wild type mice and CD45.2$^+$ knockout mice (wild type or Cybb$^{-/-}$) was isolated, RBCs were lysed using Tris-buffered ammonium chloride, and the remaining cells were quantified using a hemocytometer. CD45.1$^+$ and CD45.2$^+$ cells were then mixed equally at a 1:1 ratio, and 10^7 cells from this mixture were injected i.v. into lethally irradiated hosts that were placed on sulfatrim for 3 wk. Eight weeks later, mice were then infected by low-dose aerosol with *M. tuberculosis* H37Rv. Four weeks postinfection, the lungs of chimera mice were processed for flow cytometry. An aliquot of this suspension was saved for flow cytometry analysis of the lung population and overall bacterial levels. The remaining cells were split equally and stained with either anti-CD45.1 APC or anti-CD45.2 PE. Stained populations were then incubated with either anti-APC or anti-PE magnetic beads (Miltenyi Biotec) following the manufacturer's instructions and sorted using LS Columns (Miltenyi Biotec). Purified cells were divided equally and then plated for *M. tuberculosis* on 7H10 agar or counted and stained for analysis of cellular purity. Cells from the input homogenate, flow through, and the positive sort fractions were stained for purity with anti–CD45.1 APC, anti–CD.45.2 PE, and anti–CD11b Pacific Blue (BioLegend). Samples with >90% purity were used for subsequent analysis. At 21 d after plating, colonies were enumerated, and the *M. tuberculosis* levels per sorted cells were determined.

Quantitative real-time PCR

Cells were lysed in TRIzol LS (Thermo Fisher Scientific), and RNA was purified using Direct-zol RNA Isolation Kits (Zymogen) and quantified on NanoDrop. RNA was diluted to 5 ng/μl, and 25 ng of total RNA was used for each reaction. Ct values for each sample were determined in technical duplicates for β-Actin and IL-1β using OneStep RT-PCR Kit (Qiagen) on a Viia7 Real-Time PCR System (Life Technologies). ΔΔ Cycle threshold values were then determined for each sample.

Immunoblotting, immunoblotting quantification, and cytokine quantification

Murine cytokine concentrations in culture supernatants and cell-free lung homogenates were quantified using commercial ELISA kits (R&D Systems). All samples were normalized for total protein content. Caspase-1 activation in macrophage lysates was determined by Western blotting with Caspase-1 Ab purchased from Adipogen. Immunoblots were quantified using ImageJ software.

Results

Cybb$^{-/-}$ mice are susceptible to TB disease but maintain control of bacterial replication

To examine the role of Phox in mediating protection against *M. tuberculosis*, we compared disease progression and the immune responses in wild type and *Cybb$^{-/-}$* C57BL/6 mice postinfection via aerosol with 50–100 bacteria. We found no significant difference in the survival or bacterial levels in the lung between groups of mice up to 3 mo postinfection, confirming that Cybb is not required for surviving the early stages of *M. tuberculosis* infection (Fig. 1A, Supplemental Fig. 1). However, after 100 d of infection, *Cybb$^{-/-}$*-infected mice lost an average of 10% of their body weight, whereas wild type animals gained weight (Fig. 1B). Histopathological inspection of the lungs indicated a difference in disease between these groups, with *Cybb$^{-/-}$* lungs containing larger and less organized lesions than wild type (Fig. 1C). These data suggested that wild type and *Cybb$^{-/-}$* animals might tolerate *M. tuberculosis* infection differently even while harboring identical levels of bacteria.

To dissect the mechanisms controlling tolerance to *M. tuberculosis* disease in *Cybb$^{-/-}$* mice, we profiled the infected lungs of animals during infection by flow cytometry. We found no significant differences in the numbers of dendritic cells, macrophages, or B cells as well as total and activated T cells between wild type and *Cybb$^{-/-}$* mice (Supplemental Fig. 1). In contrast, we observed an early and sustained increase of Ly6G$^+$ CD11b$^+$ neutrophils in the infected lungs of *Cybb$^{-/-}$* mice (Fig. 1D, 1E). A 3–5-fold increase in the total number of neutrophils was observed as early as 4 wk postinfection and was maintained throughout the 12-wk study.

The cytokine IL-1β promotes neutrophil-mediated disease during *M. tuberculosis* infection of other susceptible mouse strains (10, 36). Similarly, when we assayed cytokine levels in lung homogenates, we noted a dramatic and specific increase in IL-1β concentration in *Cybb$^{-/-}$* animals compared with wild type at all time points (Fig. 1F). In contrast, no significant differences were noted for IFN-γ or TNF-α at any time point between groups (Fig. 1F). Thus, although the adaptive immune response to *M. tuberculosis* appeared to be intact, *Cybb$^{-/-}$* animals produced excess IL-1β, and the concentration of this cytokine correlated with neutrophil infiltration into the lung.

Previous studies have shown that following low-dose aerosol infection, mice deficient in Phox (both *Cybb$^{-/-}$* or Ncf1$^{-/-}$) survive for at least 60 d (24, 25). However, longer infection is likely necessary to determine whether the enhanced disease we noted in *Cybb$^{-/-}$* mice would result in a survival defect. These long-term survival experiments following low-dose aerosol proved difficult because uninfected *Cybb$^{-/-}$* mice develop arthritis as

with streptomycin. Mice were then removed from streptomycin for 3 wk halting active growth of the bacteria. (**E**) Five weeks postinfection, the total levels of viable *M. tuberculosis* in the lungs was determined by CFU plating on streptomycin (mean ± SD). (**F**) Percentage weight loss (mean change ± SD) from day 0 to day 35 was determined for wild type and *Cybb$^{-/-}$* mice. (**G**) Representative flow cytometry plot showing increased Ly6G$^+$ CD11b$^+$ neutrophil recruitment to the lungs of *Cybb$^{-/-}$* mice 5 wk postinfection (gated on live/singlets/CD45$^+$). (**H**) Quantification of neutrophil recruitment to the lungs at the indicated time points postinfection for wild type and *Cybb$^{-/-}$* mice is shown as absolute number of Ly6G$^+$ CD11b$^+$ cells per lung (mean ± SD). Data in (E)–(H) are representative of four independent experiments with four to five mice per group. *$p < 0.05$, unpaired two-tailed *t* test. (**I**) Lung homogenates from wild type or *Cybb$^{-/-}$* mice infected with 18b were probed for IL-1β by ELISA (mean ± SD). **$p < 0.01$, unpaired two-tailed *t* test. (**J**) Following low-dose aerosol infection with sfYFP H37Rv (day 0 of ∼50–100 CFU), total bacterial burden (expressed in CFU, mean ± SD) was determined in the lungs of wild type, *Cybb$^{-/-}$*, or Nos2$^{-/-}$ mice 4 wk postinfection. **$p < 0.01$, one-way ANOVA with Tukey correction. (**K**) Shown are representative flow cytometry plots from each genotype of total Ly6G$^+$ CD11b$^+$ cells in the infected lungs. (**L**) Quantification of total neutrophil recruitment to the lungs of the indicated genotypes 4 wk postinfection (mean ± SD). **$p < 0.01$, *$p < 0.05$, one-way ANOVA with Tukey correction. (**M**) Shown are representative flow cytometry plots from each genotype of infected (YFP$^+$ Ly6G$^+$ CD11b$^+$) cells in the lung. (**N**) Enumeration of infected (YFP$^+$) neutrophils (Ly6G$^+$ CD11b$^+$) or monocytes/macrophages (Ly6G- CD11b$^+$) in the indicated genotypes. Data in (J)–(N) are representative of three independent experiments with three to five mice per group. *$p < 0.05$, unpaired two-tailed *t* test.

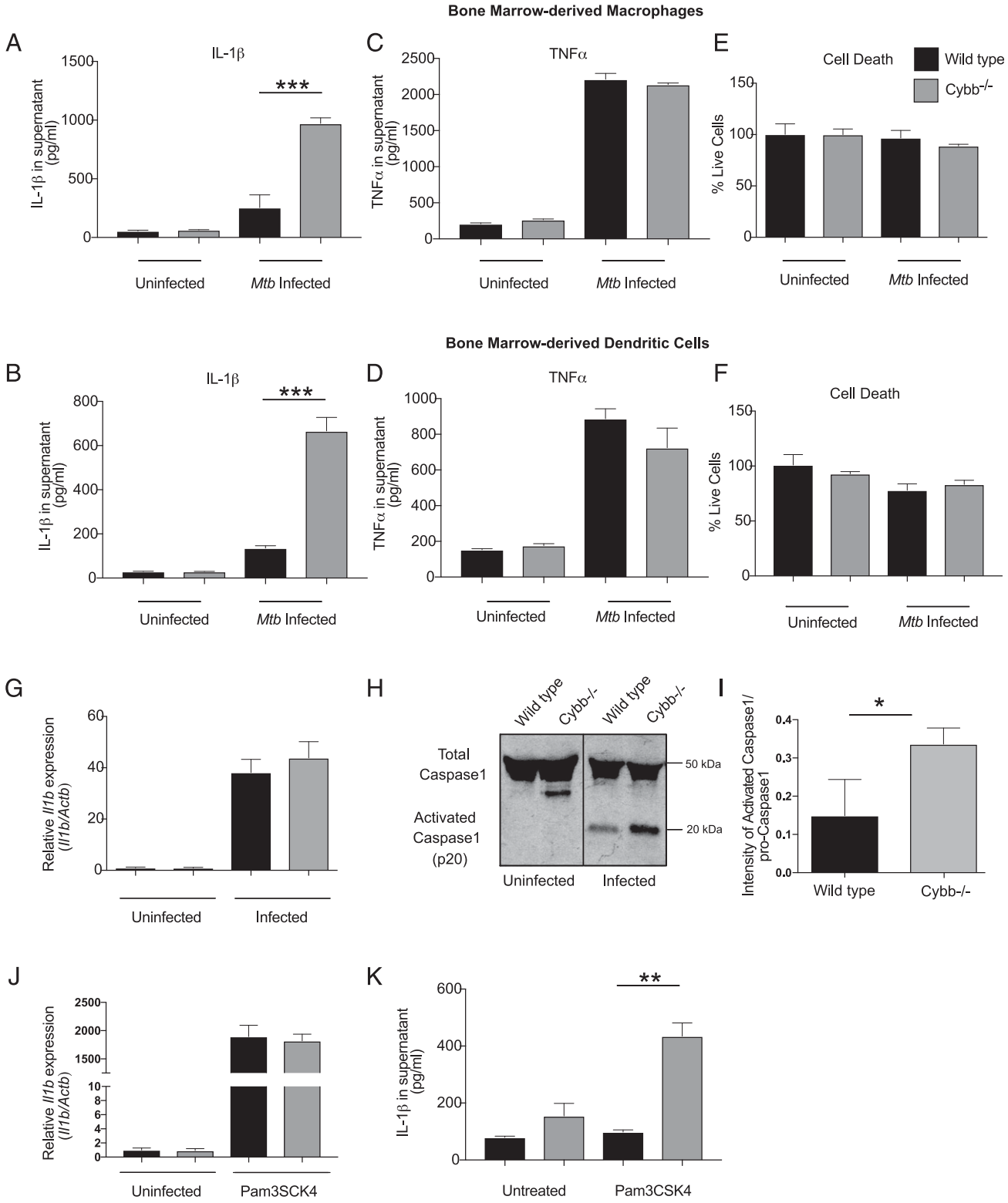

FIGURE 3. Cybb controls Caspase-1 activation in macrophages and dendritic cells during *M. tuberculosis* infection. BMDMs or BMDCs from wild type or *Cybb*$^{-/-}$ mice were left untreated or infected with *M. tuberculosis* for 4 h, then washed with fresh media. Eighteen hours later, supernatants were harvested, and the levels of (**A**) and (**B**) IL-1β and (**C**) and (**D**) TNF-α were quantified in the supernatants by ELISA. Shown is the mean of four biological replicates normalized to a standard curve ± SD ***$p < 0.001$, unpaired two-tailed *t* test. (**E**) and (**F**) Viability of remaining cells was determined by quantifying ATP via luminescence and compared with cells at 4 h postinfection (mean % viability ± SD). Data in (A), (C), and (E) are representative of five independent experiments with at least three biological replicates per experiment. Data in (B), (D), and (F) are representative of three independent experiments with four biological replicates per experiment. (**G**). Relative RNA expression of *Il1b* (compared with β-Actin) was determined from wild type and *Cybb*$^{-/-}$ BMDMs left untreated or infected for 24 h with *M. tuberculosis* (mean ± SD) by quantitative real-time PCR. Data are representative of two independent experiments with three to four biological replicates per group. (**H**) Immunoblot analysis was used to assess the activation of Caspase-1 from wild type and *Cybb*$^{-/-}$ BMDMs infected for 24 h with *M. tuberculosis*. Data are representative of three independent experiments with at least three biological replicates analyzed per experiment. (**I**) Immunoblots were quantified by comparing the intensity of activated *(Figure legend continues)*

they age (38). To avoid this confounder, we quantified the survival of mice in a shorter term study using a high-dose aerosol infection. When mice were infected with ~5000 CFU per animal, *Cybb*$^{-/-}$ mice succumbed to disease significantly more rapidly than wild type animals. *Cybb*$^{-/-}$ mice had a median survival time of 88 d, whereas only two out of 15 wild type mice succumbed during the 120-d study (Fig. 1G). To distinguish survival effects not related to *M. tuberculosis* infection, a cohort of uninfected age-matched *Cybb*$^{-/-}$ mice were maintained for the duration of the experiment. None of these animals required euthanasia over the 120 d, and no animals included in this experiment developed arthritis.

During this high-dose study, we also examined a cohort of mice 50 d postinfection and found identical levels of bacteria in the lungs and spleen between wild type and *Cybb*$^{-/-}$ groups (Fig. 1H). Consistent with our earlier findings, *Cybb*$^{-/-}$ mice showed a significant increase in neutrophils and IL-1β in the lung (Fig. 1I–K). We also found minimal levels of IL-1β and neutrophils in uninfected *Cybb*$^{-/-}$ lungs, indicating that these phenotypes are dependent on *M. tuberculosis* infection. Therefore, the loss of Cybb leads to more severe *M. tuberculosis* disease that is associated with increased IL-1β levels and neutrophil recruitment, although the number of viable *M. tuberculosis* in the lung did not appear to be affected.

Cybb controls tolerance to M. tuberculosis *infection*

Our initial results suggested that Cybb protects mice by promoting tolerance to *M. tuberculosis* infection rather than directly controlling bacterial replication. However, although viable bacterial numbers were similar in wild type and *Cybb*$^{-/-}$ mice, we could not rule out that the course of disease was altered by subtle changes in the dynamics of bacterial growth and death. To more rigorously address this question, we employed two additional animal models that allowed us to differentiate tolerance and direct antimicrobial resistance in vivo.

To more formally exclude the possibility that Cybb alters the intracellular growth of *M. tuberculosis* during infection, we used a previously optimized mixed bone marrow chimera approach (10). These experiments normalize potential inflammatory differences between wild type and *Cybb*$^{-/-}$ mice, allowing us to specifically quantify differences in bacterial control (Fig. 2A). Irradiated wild type mice were reconstituted with a 1:1 mixture of CD45.1^{+} wild type and CD45.2^{+} *Cybb*$^{-/-}$ or wild type cells. Five weeks postinfection, both CD45.1^{+} and CD45.2^{+} cells were sorted from the lungs, the levels of *M. tuberculosis* in each genotype were determined by plating, and the purity of populations was determined by flow cytometry (Fig. 2B, 2C, Supplemental Fig. 2). We found that the relative abundance of wild type and *Cybb*$^{-/-}$ cells was similarly maintained throughout infection in both the myeloid and lymphoid compartments, indicating that Cybb does not alter cellular recruitment or survival in a cell-autonomous manner. When *M. tuberculosis* was enumerated in sorted cells, we found identical levels of H37Rv in wild type CD45.1^{+} and *Cybb*$^{-/-}$ CD45.2^{+} populations from the same mouse, similar to the results from mice, where both populations were reconstituted with congenically mismatched wild type cells. In contrast, when chimeric mice were infected with a ROS-sensitive Δ*katG* mutant of *M. tuberculosis*, we found higher levels of bacteria in *Cybb*$^{-/-}$ cells compared with wild type cells from the same mouse. These data show that the assay is able to detect the cell-autonomous antimicrobial activity of ROS against a KatG-deficient *M. tuberculosis* strain, but Cybb-dependent ROS did not restrict the intracellular replication of wild type *M. tuberculosis*.

To specifically determine whether the loss of Cybb decreased tolerance to a given burden of bacteria, wild type and *Cybb*$^{-/-}$ mice were infected with a streptomycin- dependent strain of *M. tuberculosis* that allows exogenous control of bacterial replication during infection. Streptomycin is provided for the first 2 wk of infection, allowing the pathogen to reach the burden observed in a wild type *M. tuberculosis* infection. Upon streptomycin withdrawal, the pathogen is unable to replicate but remains viable and able to drive inflammatory responses (Fig. 2D) (10, 36, 39). Five weeks postinfection, *Cybb*$^{-/-}$ mice lost more weight than wild type animals while harboring identical levels of nonreplicating bacteria (Fig. 2E, 2F). Lungs from *Cybb*$^{-/-}$ mice contained significantly more neutrophils and higher levels of IL-1β compared with wild type animals (Fig. 2G–I). Thus, even when the need for antimicrobial resistance is obviated by artificially inhibiting bacterial replication, *Cybb*$^{-/-}$ animals continued to exhibit a hyperinflammatory disease.

The granulocytic inflammation observed in *Cybb*$^{-/-}$ mice was reminiscent of several other susceptible mouse strains. However, the neutrophil recruitment in other models is generally associated with a concomitant increase in bacterial growth (40–42) and a transition of the intracellular *M. tuberculosis* burden from macrophages to granulocytes (10). We hypothesized that *Cybb*$^{-/-}$ mice may be able to retain control of *M. tuberculosis* replication because the bacteria remain in macrophages. To test this hypothesis, we used a YFP-expressing *M. tuberculosis* strain to compare the distribution of cells harboring bacteria in wild type and *Cybb*$^{-/-}$ mice with *Nos2*$^{-/-}$ animals in which *M. tuberculosis* replicates to high numbers in association with infiltrating granulocytes (10). Four weeks postinfection, we found that lungs from both *Cybb*$^{-/-}$ and *Nos2*$^{-/-}$ mice contain higher levels of IL-1β and neutrophils than wild type animals, although the loss of *Nos2*$^{-/-}$ produced a much more severe phenotype than *Cybb*$^{-/-}$ (Fig. 2J–L, Supplemental Fig. 2). However, the cells harboring *M. tuberculosis* in these two susceptible mouse strains differed. In wild type and *Cybb*$^{-/-}$ mice, YFP-*M. tuberculosis* was evenly distributed between CD11b^{+}/Ly6G^{+} neutrophils and the CD11b^{+}/Ly6G^{-} population that consists of macrophages and dendritic cells (43). This proportion was dramatically altered in *Nos2*$^{-/-}$ mice, where close to 90% of bacteria were found in the neutrophil compartment (Fig. 2M, 2N). Thus, unlike other susceptible mouse models, the loss of Cybb does not alter bacterial replication or the distribution of *M. tuberculosis* in different myeloid subsets. Instead, this gene plays a specific role in controlling IL-1β activation, neutrophil recruitment to the infected lung, and disease progression. As a result, we conclude that Cybb specifically promotes tolerance to *M. tuberculosis* infection.

p20–Caspase-1 to total pro–Caspase-1 bands. Quantification was done on three biological replicates. *$p < 0.05$, unpaired two-tailed *t* test. (**J**) Relative RNA expression of *Il1b* (compared with *Actb*) was determined from wild type and *Cybb*$^{-/-}$ BMDMs left untreated or treated with Pam3CSK4 for 24 h (mean ± SD) by quantitative real-time PCR. Data are representative of two independent experiments with three to four biological replicates per group. (**K**) Wild type and *Cybb*$^{-/-}$ BMDMs were left untreated or treated with PAM3CSK4 for 12 h, supernatants were harvested, and the levels of IL-1β were quantified by ELISA (mean ± SD). Data are representative of three independent experiments with four biological replicates per experiment. **$p < 0.01$, unpaired two-tailed *t* test.

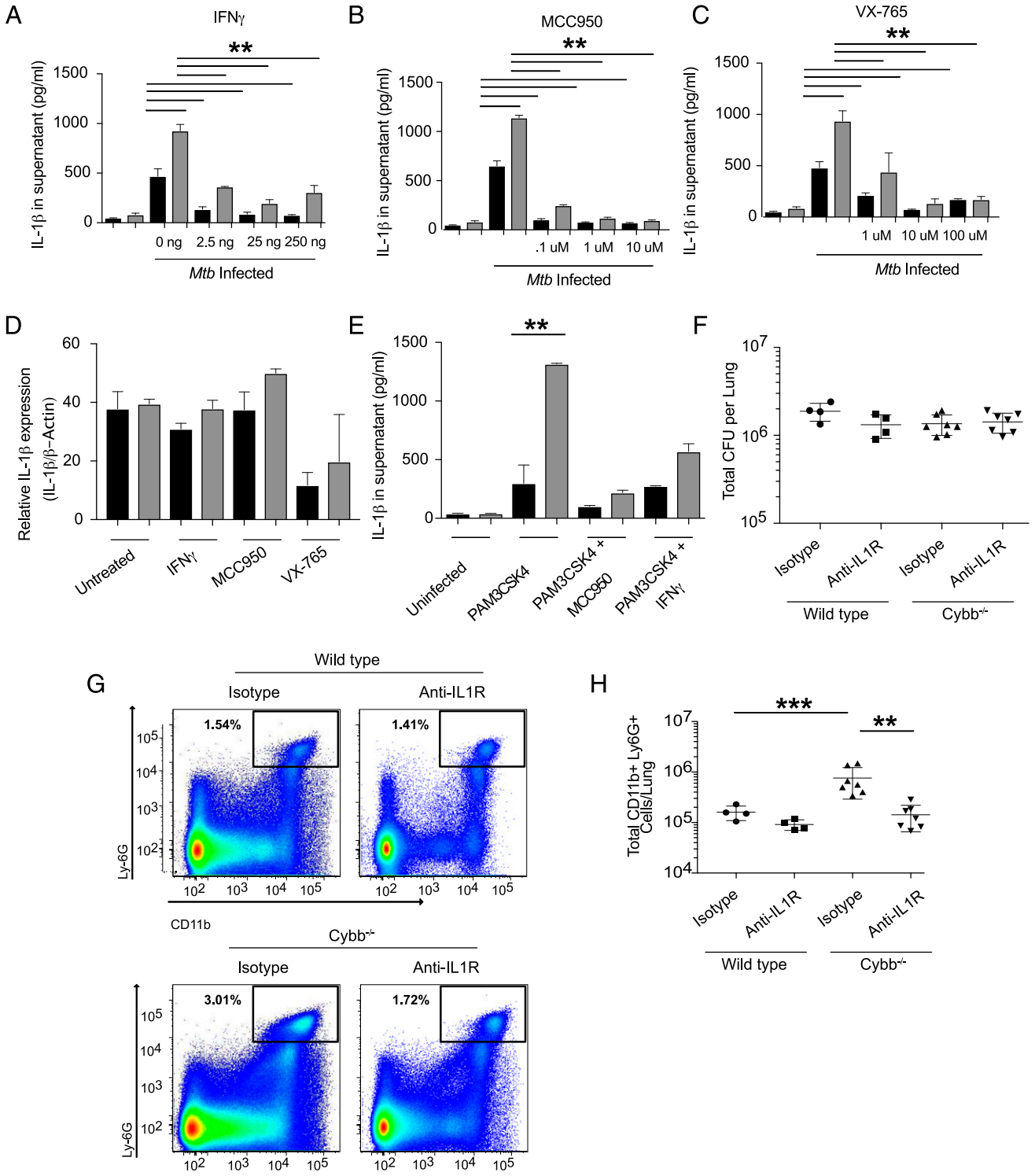

FIGURE 4. Hyperinflammation in *Cybb*$^{-/-}$ is reversed by inflammasome and IL-1 inhibition. (**A**) Wild type (black bars) and *Cybb*$^{-/-}$ (gray bars) BMDMs were left untreated or treated with the indicated concentrations of IFN-γ for 12 h. Cells were then infected with *M. tuberculosis* for 4 h, then washed with fresh media. Eighteen hours later, supernatants were harvested, and levels of IL-1β from each condition were quantified by ELISA (mean ± SD). Data are representative of three independent experiments with at least three biological replicates per experiment. $^{**}p < 0.01$, one-way ANOVA with Tukey correction. (**B**) Wild type and *Cybb*$^{-/-}$ BMDMs were left untreated or treated with the indicated concentrations of MCC950 for 2 h. Cells were then infected with *M. tuberculosis* for 4 h, then washed with fresh media with inhibitor. Eighteen hours later, supernatants were harvested, and levels of IL-1β from each condition were quantified by ELISA (mean ± SD). Data are representative of three independent experiments with at least three biological replicates per experiment. $^{**}p < 0.01$, one-way ANOVA with Tukey correction. (**C**) Wild type and *Cybb*$^{-/-}$ BMDMs were left untreated or treated with the indicated concentrations of VX-765 for 2 h. Cells were then infected with *M. tuberculosis* for 4 h, then washed with fresh media with inhibitor. Eighteen hours later, supernatants were harvested, and levels of IL-1β from each condition were quantified by ELISA (mean ± SD). Data are representative of three independent experiments with at least three biological replicates per experiment. $^{**}p < 0.01$, one-way ANOVA with Tukey correction. (**D**) Relative RNA expression of IL-1β (compared with b-Actin) was determined from wild type and *Cybb*$^{-/-}$ BMDMs left infected for 24 h with *M. tuberculosis* in the presence or absence of the indicated inhibitors (mean ± SD) by quantitative real-time PCR. Data are representative of two experiments with four biological replicates per group. (**E**) Wild type and *Cybb*$^{-/-}$ BMDMs were left untreated or treated with 25 ng/ml *(Figure legend continues)*

Enhanced IL-1β activation by Cybb$^{-/-}$ macrophages and dendritic cells is caused by deregulated Caspase-1 inflammasome activation

To investigate the mechanism underlying increased IL-1β production in *Cybb*$^{-/-}$ mice, we quantified the release of mature cytokine from BMDMs and BMDCs. Compared with wild type, we found that *Cybb*$^{-/-}$ BMDMs and BMDCs produced 4–5-fold more IL-1β after 24 h of *M. tuberculosis* infection (Fig. 3A, 3B). Under these conditions, wild type and *Cybb*$^{-/-}$ cells remained equally viable and produced equivalent amounts of TNF (Fig. 3C–F), suggesting that the effect of Cybb on IL-1β activation was specific to this cytokine.

The release of mature IL-1β requires two distinct signals (44). The first signal induces the expression of *Il1b* mRNA and subsequent translation of pro–IL-1β, and a second signal activates Caspase-1, which is necessary for the processing and secretion of mature IL-1β. To understand what step of IL-1β production was altered in *Cybb*$^{-/-}$ cells, we quantified these two signals. The expression of *Il1b* mRNA in uninfected and infected BMDMs was unchanged between wild type and *Cybb*$^{-/-}$ BMDMs (Fig. 3G). In contrast, under the same conditions, the processing of Caspase-1 to its active form was increased in infected *Cybb*$^{-/-}$ BMDMs compared with wild type cells (Fig. 3H, 3I).

These observations suggested that Caspase-1 activity is increased in *Cybb*$^{-/-}$ cells, which could allow mature IL-1β secretion in the absence of an inflammasome activator. To test this hypothesis, we stimulated cells with the TLR2 agonist PAM3CSK4 to induce pro–IL-1β expression. PAM3CSK4 stimulation induced *Il1b* mRNA to similar levels between wild type and *Cybb*$^{-/-}$ BMDMs, albeit over 100 times higher than infection with *M. tuberculosis* (Fig. 3J). In wild type cells, this induction of *Il1b* expression produced little mature IL-1β secretion, consistent with the need for subsequent inflammasome activation. In contrast, induction of *Il1b* expression led to robust secretion of mature IL-1β from *Cybb*$^{-/-}$ BMDM, consistent with unregulated inflammasome activity in these cells (Fig. 3K). Together, these data show that loss of Cybb leads to hyperactivation of Caspase-1 and increased release of IL-1β during *M. tuberculosis* infection of both BMDMs and BMDCs.

Loss of tolerance is reversed in Cybb$^{-/-}$ macrophages and mice by blocking the production or activity of IL-1β

The NLRP3 inflammasome consists of NLRP3, ASC, and Caspase-1. Although this complex is generally responsible for IL-1β processing in *M. tuberculosis*–infected macrophages (45, 46), it remained unclear whether the enhanced IL-1β secretion from *Cybb*$^{-/-}$ cells also relied on these components. To identify the responsible complex, we blocked the activation of the NLRP3 inflammasome in several distinct ways. The NLRP3 inflammasome is specifically inhibited by IFN-γ stimulation via the NO-dependent nitrosylation of the NLRP3 protein (36). Pretreatment of wild type and *Cybb*$^{-/-}$ BMDMs with various concentrations of IFN-γ inhibited the secretion of mature IL-1β from both wild type and *Cybb*$^{-/-}$ BMDMs compared with untreated cells. Although this result indicated an important role for NLRP3, IFN-γ pretreatment did not completely suppress IL-1β secretion, and there remained significant differences in the IL-1β release between *Cybb*$^{-/-}$ and wild type cells at all concentrations of the cytokine (Fig. 4A).

To more directly assess the role of NLRP3 and Caspase-1 in IL-1β maturation in *Cybb*$^{-/-}$ cells, we employed specific small molecule inhibitors. Treatment of *M. tuberculosis*–infected BMDMs with either the NLRP3 inhibitor MCC950 (45) or the Caspase-1 inhibitor VX-765 (47) caused a dramatic reduction in IL-1β in both wild type and *Cybb*$^{-/-}$ BMDMs compared with untreated cells (Fig. 4B, 4C). This 10-fold decrease in IL-1β secretion could not be attributed to inhibition of pro–IL-1β levels, as none of these inhibitors affected *Il1b* mRNA by more than 2-fold. Similarly, the spontaneous IL-1β secretion observed upon PAM3CSK4 stimulation was also inhibited by MCC950 and IFN-γ (Fig. 4E). In each case, inflammasome inhibition reduced IL-1β secretion to the same level in both wild type and *Cybb*$^{-/-}$ cells, indicating that the NLRP3 inflammasome was responsible for the enhanced processing and secretion of this cytokine in *Cybb*$^{-/-}$ BMDM.

Based on these studies, we hypothesized that the tolerance defect observed in the intact mouse was due to inflammasome-dependent IL-1 signaling. The contributions of IL-1β during *M. tuberculosis* infection are complex (48, 49). Production of this cytokine is important for antimicrobial immunity, but persistent IL-1 signaling can promote pathologic condition. To focus on the role of overproduction of IL-1β on tolerance, we inhibited IL-1 signaling in mice infected with nonreplicating streptomycin-dependent *M. tuberculosis* to normalize the bacterial burden. Two weeks postinfection, wild type and *Cybb*$^{-/-}$ mice were treated with either an isotype control Ab or an anti–IL-1R Ab to block the effect of increased IL-1β activity. As expected, *M. tuberculosis* levels were similar in all mice, but more neutrophils accumulated in the lungs of *Cybb*$^{-/-}$ animals (Fig. 4F–H). Although anti–IL-1R treatment had no effect in wild type animals, inhibition of IL-1 signaling reduced neutrophil infiltration in *Cybb*$^{-/-}$ mice to the level observed in wild type animals. Taken together, our data show that *Cybb*$^{-/-}$ contributes to protective immunity to *M. tuberculosis* not by controlling bacterial replication but instead by preventing an IL-1–dependent inflammatory response that increases neutrophil recruitment to the lung and exacerbates disease progression.

Discussion

The role of the Phox complex in protection from TB has presented a paradox (34). Based on the well-described antimicrobial properties of Phox-derived ROS, previous studies have focused on examining the function of Phox components in controlling *M. tuberculosis* replication in mice (24, 25, 50). The lack of long-term differences in bacterial levels observed in these studies suggested that Phox may not play a strong antimicrobial role during *M. tuberculosis*

IFN-γ or 1 μM MCC950 overnight. The following day, cells were treated with PAM3CSK4 for 12 h, supernatants were harvested, and the levels of IL-1β were quantified by ELISA (mean ± SD). Data are representative of two independent experiments with four biological replicates per experiment. $^{**}p < 0.01$ by unpaired two-tailed *t* test. (**F**) Wild type and *Cybb*$^{-/-}$ mice were infected intratracheally with *M. tuberculosis* strain 18b and treated for 2 wk daily with streptomycin, then injected every other day for 2 wk with 200 μg of either isotype control Ab or anti–IL-1R Ab. The total levels of viable *M. tuberculosis* in the lungs was determined by CFU plating on streptomycin (mean ± SD) with four to seven mice per group. (**G**) Representative flow cytometry plot showing Ly6G$^+$ CD11b$^+$ neutrophil recruitment to the lungs of *Cybb*$^{-/-}$ mice during control and IL-1R blockade conditions (gated on live/singlets/CD45$^+$). (**H**) Quantification of neutrophil recruitment to the lungs at the indicated time points postinfection for wild type and *Cybb*$^{-/-}$ mice during control and IL-1R blockade conditions is shown as an absolute number of Ly6G$^+$ CD11b$^+$ cells per lung (mean ± SD). Data in (F) and (G) are representative of two independent experiments with four to seven mice per group. $^{***}p < 0.001$, $^{**}p < 0.01$, one-way ANOVA with Tukey correction.

infection. Our dissection of disease progression in Cybb-deficient mice shows that Phox plays no discernable role in antimicrobial resistance to *M. tuberculosis* over long-term infections. However, we uncovered a previously unknown role for this complex in promoting tolerance to *M. tuberculosis* infection and inhibiting TB disease.

Although we were able to clearly delineate the role of Phox during *M. tuberculosis* infection, the role(s) played by this complex in any given infection is likely to vary. Phox-deficient mice are unable to control the growth of several bacterial pathogens that are known to cause serious infections in CGD patients, including non-TB mycobacteria (50–53). In the context of these infections, the antimicrobial functions of Phox may predominate. In fact, several studies suggest an important role for Phox in controlling replication of pathogenic mycobacteria other than *M. tuberculosis*. High-dose i.v. or intratracheal infection with *M. avium*, *M. marinum*, and *M. bovis* BCG all produce higher bacterial burdens and more severe disease in Phox-deficient mice than wild type animals (50, 53, 54). Although these observations indicate that Phox can play an antimicrobial role in these infections, the specific role of this complex in promoting tolerance could not be discerned because of the difference in bacterial numbers in wild type and mutant animals.

The differential dependency on Phox for antimicrobial resistance to *M. tuberculosis* versus these other mycobacterial species likely reflects a differential susceptibility to ROS-mediated killing. Several studies support this model by demonstrating that mechanisms by which neutrophils kill these different organisms are distinct. Neutrophil-mediated killing of *M. tuberculosis* is independent of Phox-derived ROS, as neutrophils from CGD patients show no defect in *M. tuberculosis* killing, and inhibitors of ROS do not alter this activity (55, 56). In contrast, *M. marinum* is killed by neutrophils in a ROS-dependent manner (57). Similarly, neutrophil depletion promotes the growth of BCG in the lung but has little effect in the context of *M. tuberculosis* (10, 58). This effect can be explained based on the ability of the ESX-1 secretion system, which is absent from BCG, to inhibit neutrophil killing (59). Based on these differences in susceptibility to neutrophil killing, we speculate that Phox-derived ROS may contribute to both tolerance and resistance to mycobacteria, such as *M. avium* or *M. bovis* BCG, but this remains to be rigorously tested. For a pathogen such as *M. tuberculosis* that is resistant to ROS-mediated toxicity and persists in the tissue to promote continual inflammatory damage, the tolerance-promoting activity of Phox predominates.

During *M. tuberculosis* infection, we found that the ROS produced by Phox are critical to control the activation of the NLRP3 inflammasome. In contrast, mitochondrial ROS are well known to activate inflammatory cascades (60), suggesting that the context by which ROS are produced influences the inflammatory outcome of activated cells. Despite this complexity, Phox-deficient mice and CGD patients suffer from hyperinflammatory diseases, including arthritis, colitis, and prolonged inflammatory reactions to microbial products, indicating that the dominant immunoregulatory role for Phox-derived ROS is anti-inflammatory (61–63). Although the noninfectious granulomatous lesions of CGD patients are typified by mononuclear infiltrate, the histopathology of infectious foci are more variable. Pulmonary infections generally produce either pneumonia or abscess, which might resemble the neutrophil-associated disease that we observe in mice (64).

CGD patients are more likely to develop disseminated BCG infections following vaccination. Although it is likely that *M. bovis* is differentially susceptible to ROS killing as discussed above, it is also possible that enhanced inflammasome activation contributes to this disease. Although inflammasome activation in wild type animals requires the ESX-1 secretion system that is deleted in BCG, we observed robust stimulation of inflammasome activation in Phox-deficient cells treated with TLR stimulation alone. These results suggest that activation of Caspase-1 may occur in Phox-deficient cells even upon infection with ESX-1–deficient pathogens.

Several nonmutually exclusive mechanisms could explain the anti-inflammatory effect of Phox-derived ROS. For example, ROS has been proposed to inhibit the production of inflammatory mediators by inhibiting autophagy (65). In the absence of ROS, the reduced levels of autophagy may drive enhanced inflammasome activation. Another mechanism was described in superoxide dismutase1 (*Sod1*)–deficient cells, where the accumulation of ROS inhibits Caspase-1 activation through glutathionation of reactive cysteines (66). It is possible that the loss of ROS leads to loss of glutathionation and subsequently results in the hyperactivation of Caspase-1. This latter mechanism is reminiscent of the process by which NO inhibits inflammasome activation via S-nitrosylation of NLRP3 (36). The intersection of these two important anti-inflammatory pathways at the NLRP3 inflammasome indicates that this complex may be a critical point of integration where inflammatory cascades are controlled during chronic infections.

Our findings are consistent with a growing body of literature suggesting that inflammasome-derived IL-1 promotes TB disease progression. For example, genetic polymorphisms that increase the expression of IL-1β or the production of IL-1–dependent proinflammatory lipid mediators are associated with TB disease progression (10, 67). Similarly, transcriptional signatures of inflammasome activation have been observed in severe forms of TB disease, such as meningitis (68) and TB-associated immune reconstitution syndrome (69). Together with our work, these findings imply that a failure in tolerance alone can compromise protective immunity to *M. tuberculosis*, even in the context of fully functional antimicrobial resistance responses, and that Caspase-1 represents a critical point at which tolerance is regulated.

Acknowledgments

We are thankful to members of the Sassetti, Behar, and Fitzgerald laboratory for helpful discussions.

Disclosures

The authors have no financial conflicts of interest.

References

1. Medzhitov, R., D. S. Schneider, and M. P. Soares. 2012. Disease tolerance as a defense strategy. *Science* 335: 936–941.
2. Schneider, D. S., and J. S. Ayres. 2008. Two ways to survive infection: what resistance and tolerance can teach us about treating infectious diseases. *Nat. Rev. Immunol.* 8: 889–895.
3. Olive, A. J., and C. M. Sassetti. 2016. Metabolic crosstalk between host and pathogen: sensing, adapting and competing. *Nat. Rev. Microbiol.* 14: 221–234.
4. Pilla-Moffett, D., M. F. Barber, G. A. Taylor, and J. Coers. 2016. Interferon-inducible GTPases in host resistance, inflammation and disease. *J. Mol. Biol.* 428: 3495–3513.
5. Hood, M. I., and E. P. Skaar. 2012. Nutritional immunity: transition metals at the pathogen-host interface. *Nat. Rev. Microbiol.* 10: 525–537.
6. Ayres, J. S., and D. S. Schneider. 2008. A signaling protease required for melanization in Drosophila affects resistance and tolerance of infections. *PLoS Biol.* 6: 2764–2773.
7. Weis, S., A. R. Carlos, M. R. Moita, S. Singh, B. Blankenhaus, S. Cardoso, R. Larsen, S. Rebelo, S. Schauble, L. Del Barrio, et al. 2017. Metabolic adaptation establishes disease tolerance to sepsis. *Cell* 169: 1263–1275.e14.
8. Jamieson, A. M., L. Pasman, S. Yu, P. Gamradt, R. J. Homer, T. Decker, and R. Medzhitov. 2013. Role of tissue protection in lethal respiratory viral-bacterial coinfection. *Science* 340: 1230–1234.
9. Jeney, V., S. Ramos, M. L. Bergman, I. Bechmann, J. Tischer, A. Ferreira, V. Oliveira-Marques, C. J. Janse, S. Rebelo, S. Cardoso, and M. P. Soares. 2014. Control of disease tolerance to malaria by nitric oxide and carbon monoxide. *Cell Rep.* 8: 126–136.

10. Mishra, B. B., R. R. Lovewell, A. J. Olive, G. Zhang, W. Wang, E. Eugenin, C. M. Smith, J. Y. Phuah, J. E. Long, M. L. Dubuke, et al. 2017. Nitric oxide prevents a pathogen-permissive granulocytic inflammation during tuberculosis. *Nat. Microbiol.* 2: 17072.
11. Meunier, I., E. Kaufmann, J. Downey, and M. Divangahi. 2017. Unravelling the networks dictating host resistance versus tolerance during pulmonary infections. *Cell Tissue Res.* 367: 525–536.
12. Cadena, A. M., S. M. Fortune, and J. L. Flynn. 2017. Heterogeneity in tuberculosis. *Nat. Rev. Immunol.* 17: 691–702.
13. Chen, R. Y., L. E. Dodd, M. Lee, P. Paripati, D. A. Hammoud, J. M. Mountz, D. Jeon, N. Zia, H. Zahiri, M. T. Coleman, et al. 2014. PET/CT imaging correlates with treatment outcome in patients with multidrug-resistant tuberculosis. *Sci. Transl. Med.* 6: 265ra166.
14. Tobin, D. M., F. J. Roca, S. F. Oh, R. McFarland, T. W. Vickery, J. P. Ray, D. C. Ko, Y. Zou, N. D. Bang, T. T. Chau, et al. 2012. Host genotype-specific therapies can optimize the inflammatory response to mycobacterial infections. *Cell* 148: 434–446.
15. López, B., D. Aguilar, H. Orozco, M. Burger, C. Espitia, V. Ritacco, L. Barrera, K. Kremer, R. Hernandez-Pando, K. Huygen, and D. van Soolingen. 2003. A marked difference in pathogenesis and immune response induced by different *Mycobacterium tuberculosis* genotypes. *Clin. Exp. Immunol.* 133: 30–37.
16. Redford, P. S., P. J. Murray, and A. O'Garra. 2011. The role of IL-10 in immune regulation during *M. tuberculosis* infection. *Mucosal Immunol.* 4: 261–270.
17. Larson, R. P., S. Shafiani, and K. B. Urdahl. 2013. Foxp3(+) regulatory T cells in tuberculosis. *Adv. Exp. Med. Biol.* 783: 165–180.
18. Jayaraman, P., M. K. Jacques, C. Zhu, K. M. Steblenko, B. L. Stowell, A. Madi, A. C. Anderson, V. K. Kuchroo, and S. M. Behar. 2016. TIM3 mediates T cell exhaustion during *Mycobacterium tuberculosis* infection. *PLoS Pathog.* 12: e1005490.
19. Desvignes, L., C. Weidinger, P. Shaw, M. Vaeth, T. Ribierre, M. Liu, T. Fergus, L. Kozhaya, L. McVoy, D. Unutmaz, et al. 2015. STIM1 controls T cell-mediated immune regulation and inflammation in chronic infection. *J. Clin. Invest.* 125: 2347–2362.
20. Pasipanodya, J. G., S. J. McNabb, P. Hilsenrath, S. Bae, K. Lykens, E. Vecino, G. Munguia, T. L. Miller, G. Drewyer, and S. E. Weis. 2010. Pulmonary impairment after tuberculosis and its contribution to TB burden. *BMC Public Health* 10: 259.
21. Segal, A. W. 2005. How neutrophils kill microbes. *Annu. Rev. Immunol.* 23: 197–223.
22. Panday, A., M. K. Sahoo, D. Osorio, and S. Batra. 2015. NADPH oxidases: an overview from structure to innate immunity-associated pathologies. *Cell. Mol. Immunol.* 12: 5–23.
23. Johnston, R. B., Jr., and R. L. Baehner. 1970. Improvement of leukocyte bactericidal activity in chronic granulomatous disease. *Blood* 35: 350–355.
24. Cooper, A. M., B. H. Segal, A. A. Frank, S. M. Holland, and I. M. Orme. 2000. Transient loss of resistance to pulmonary tuberculosis in p47(phox$^{-/-}$) mice. *Infect. Immun.* 68: 1231–1234.
25. Jung, Y. J., R. LaCourse, L. Ryan, and R. J. North. 2002. Virulent but not avirulent *Mycobacterium tuberculosis* can evade the growth inhibitory action of a T helper 1-dependent, nitric oxide Synthase 2-independent defense in mice. *J. Exp. Med.* 196: 991–998.
26. Ng, V. H., J. S. Cox, A. O. Sousa, J. D. MacMicking, and J. D. McKinney. 2004. Role of KatG catalase-peroxidase in mycobacterial pathogenesis: countering the phagocyte oxidative burst. *Mol. Microbiol.* 52: 1291–1302.
27. Colangeli, R., A. Haq, V. L. Arcus, E. Summers, R. S. Magliozzo, A. McBride, A. K. Mitra, M. Radjainia, A. Khajo, W. R. Jacobs, Jr., et al. 2009. The multifunctional histone-like protein Lsr2 protects mycobacteria against reactive oxygen intermediates. *Proc. Natl. Acad. Sci. USA* 106: 4414–4418.
28. Nambi, S., J. E. Long, B. B. Mishra, R. Baker, K. C. Murphy, A. J. Olive, H. P. Nguyen, S. A. Shaffer, and C. M. Sassetti. 2015. The oxidative stress network of *Mycobacterium tuberculosis* reveals coordination between radical detoxification systems. *Cell Host Microbe* 17: 829–837.
29. Köster, S., S. Upadhyay, P. Chandra, K. Papavinasasundaram, G. Yang, A. Hassan, S. J. Grigsby, E. Mittal, H. S. Park, V. Jones, et al. 2017. *Mycobacterium tuberculosis* is protected from NADPH oxidase and LC3-associated phagocytosis by the LCP protein CpsA. [Published erratum appears in 2017 *Proc. Natl. Acad. Sci. USA* 114: E9752.] *Proc. Natl. Acad. Sci. USA* 114: E8711–E8720.
30. Nathan, C., and M. U. Shiloh. 2000. Reactive oxygen and nitrogen intermediates in the relationship between mammalian hosts and microbial pathogens. *Proc. Natl. Acad. Sci. USA* 97: 8841–8848.
31. Bustamante, J., A. A. Arias, G. Vogt, C. Picard, L. B. Galicia, C. Prando, A. V. Grant, C. C. Marchal, M. Hubeau, A. Chapgier, et al. 2011. Germline CYBB mutations that selectively affect macrophages in kindreds with X-linked predisposition to tuberculous mycobacterial disease. *Nat. Immunol.* 12: 213–221.
32. Khan, T. A., K. Kalsoom, A. Iqbal, H. Asif, H. Rahman, S. O. Farooq, H. Naveed, U. Nasir, M. U. Amin, M. Hussain, et al. 2016. A novel missense mutation in the NADPH binding domain of CYBB abolishes the NADPH oxidase activity in a male patient with increased susceptibility to infections. *Microb. Pathog.* 100: 163–169.
33. Lee, P. P., K. W. Chan, L. Jiang, T. Chen, C. Li, T. L. Lee, P. H. Mak, S. F. Fok, X. Yang, and Y. L. Lau. 2008. Susceptibility to mycobacterial infections in children with X-linked chronic granulomatous disease: a review of 17 patients living in a region endemic for tuberculosis. *Pediatr. Infect. Dis. J.* 27: 224–230.
34. Deffert, C., J. Cachat, and K. H. Krause. 2014. Phagocyte NADPH oxidase, chronic granulomatous disease and mycobacterial infections. *Cell. Microbiol.* 16: 1168–1178.
35. Lau, Y. L., G. C. Chan, S. Y. Ha, Y. F. Hui, and K. Y. Yuen. 1998. The role of phagocytic respiratory burst in host defense against *Mycobacterium tuberculosis*. *Clin. Infect. Dis.* 26: 226–227.
36. Mishra, B. B., V. A. Rathinam, G. W. Martens, A. J. Martinot, H. Kornfeld, K. A. Fitzgerald, and C. M. Sassetti. 2013. Nitric oxide controls the immunopathology of tuberculosis by inhibiting NLRP3 inflammasome-dependent processing of IL-1β. *Nat. Immunol.* 14: 52–60.
37. Zanoni, I., Y. Tan, M. Di Gioia, A. Broggi, J. Ruan, J. Shi, C. A. Donado, F. Shao, H. Wu, J. R. Springstead, and J. C. Kagan. 2016. An endogenous caspase-11 ligand elicits interleukin-1 release from living dendritic cells. *Science* 352: 1232–1236.
38. Lee, K., H. Y. Won, M. A. Bae, J. H. Hong, and E. S. Hwang. 2011. Spontaneous and aging-dependent development of arthritis in NADPH oxidase 2 deficiency through altered differentiation of CD11b+ and Th/Treg cells. *Proc. Natl. Acad. Sci. USA* 108: 9548–9553.
39. Honoré, N., G. Marchal, and S. T. Cole. 1995. Novel mutation in 16S rRNA associated with streptomycin dependence in *Mycobacterium tuberculosis*. *Antimicrob. Agents Chemother.* 39: 769–770.
40. Kimmey, J. M., J. P. Huynh, L. A. Weiss, S. Park, A. Kambal, J. Debnath, H. W. Virgin, and C. L. Stallings. 2015. Unique role for ATG5 in neutrophil-mediated immunopathology during *M. tuberculosis* infection. *Nature* 528: 565–569.
41. Kramnik, I., W. F. Dietrich, P. Demant, and B. R. Bloom. 2000. Genetic control of resistance to experimental infection with virulent *Mycobacterium tuberculosis*. *Proc. Natl. Acad. Sci. USA* 97: 8560–8565.
42. Nandi, B., and S. M. Behar. 2011. Regulation of neutrophils by interferon-γ limits lung inflammation during tuberculosis infection. *J. Exp. Med.* 208: 2251–2262.
43. Wolf, A. J., B. Linas, G. J. Trevejo-Nuñez, E. Kincaid, T. Tamura, K. Takatsu, and J. D. Ernst. 2007. *Mycobacterium tuberculosis* infects dendritic cells with high frequency and impairs their function in vivo. *J. Immunol.* 179: 2509–2519.
44. von Moltke, J., J. S. Ayres, E. M. Kofoed, J. Chavarría-Smith, and R. E. Vance. 2013. Recognition of bacteria by inflammasomes. *Annu. Rev. Immunol.* 31: 73–106.
45. Coll, R. C., A. A. Robertson, J. J. Chae, S. C. Higgins, R. Muñoz-Planillo, M. C. Inserra, I. Vetter, L. S. Dungan, B. G. Monks, A. Stutz, et al. 2015. A small-molecule inhibitor of the NLRP3 inflammasome for the treatment of inflammatory diseases. *Nat. Med.* 21: 248–255.
46. Dorhoi, A., G. Nouailles, S. Jörg, K. Hagens, E. Heinemann, L. Pradl, D. Oberbeck-Müller, M. A. Duque-Correa, S. T. Reece, J. Ruland, et al. 2012. Activation of the NLRP3 inflammasome by *Mycobacterium tuberculosis* is uncoupled from susceptibility to active tuberculosis. *Eur. J. Immunol.* 42: 374–384.
47. Stack, J. H., K. Beaumont, P. D. Larsen, K. S. Straley, G. W. Henkel, J. C. Randle, and H. M. Hoffman. 2005. IL-converting enzyme/caspase-1 inhibitor VX-765 blocks the hypersensitive response to an inflammatory stimulus in monocytes from familial cold autoinflammatory syndrome patients. *J. Immunol.* 175: 2630–2634.
48. Mayer-Barber, K. D., D. L. Barber, K. Shenderov, S. D. White, M. S. Wilson, A. Cheever, D. Kugler, S. Hieny, P. Caspar, G. Núñez, et al. 2010. Caspase-1 independent IL-1beta production is critical for host resistance to *Mycobacterium tuberculosis* and does not require TLR signaling in vivo. *J. Immunol.* 184: 3326–3330.
49. Nunes-Alves, C., M. G. Booty, S. M. Carpenter, P. Jayaraman, A. C. Rothchild, and S. M. Behar. 2014. In search of a new paradigm for protective immunity to TB. *Nat. Rev. Microbiol.* 12: 289–299.
50. Deffert, C., M. G. Schäppi, J. C. Pache, J. Cachat, D. Vesin, R. Bisig, X. Ma Mulone, T. Kelkka, R. Holmdahl, I. Garcia, et al. 2014. *Bacillus* calmette-guerin infection in NADPH oxidase deficiency: defective mycobacterial sequestration and granuloma formation. *PLoS Pathog.* 10: e1004325.
51. Jackson, S. H., J. I. Gallin, and S. M. Holland. 1995. The p47phox mouse knockout model of chronic granulomatous disease. *J. Exp. Med.* 182: 751–758.
52. Dinauer, M. C., M. B. Deck, and E. R. Unanue. 1997. Mice lacking reduced nicotinamide adenine dinucleotide phosphate oxidase activity show increased susceptibility to early infection with *Listeria monocytogenes*. *J. Immunol.* 158: 5581–5583.
53. Fujita, M., E. Harada, T. Matsumoto, Y. Mizuta, S. Ikegame, H. Ouchi, I. Inoshima, S. Yoshida, K. Watanabe, and Y. Nakanishi. 2010. Impaired host defence against *Mycobacterium avium* in mice with chronic granulomatous disease. *Clin. Exp. Immunol.* 160: 457–460.
54. Chao, W. C., C. L. Yen, C. Y. Hsieh, Y. F. Huang, Y. L. Tseng, P. A. Nigrovic, and C. C. Shieh. 2017. Mycobacterial infection induces higher interleukin-1β and dysregulated lung inflammation in mice with defective leukocyte NADPH oxidase. *PLoS One* 12: e0189453.
55. Jones, G. S., H. J. Amirault, and B. R. Andersen. 1990. Killing of *Mycobacterium tuberculosis* by neutrophils: a nonoxidative process. *J. Infect. Dis.* 162: 700–704.
56. Kisich, K. O., M. Higgins, G. Diamond, and L. Heifets. 2002. Tumor necrosis factor alpha stimulates killing of *Mycobacterium tuberculosis* by human neutrophils. *Infect. Immun.* 70: 4591–4599.
57. Yang, C. T., C. J. Cambier, J. M. Davis, C. J. Hall, P. S. Crosier, and L. Ramakrishnan. 2012. Neutrophils exert protection in the early tuberculous granuloma by oxidative killing of mycobacteria phagocytosed from infected macrophages. *Cell Host Microbe* 12: 301–312.
58. Fulton, S. A., S. M. Reba, T. D. Martin, and W. H. Boom. 2002. Neutrophil-mediated mycobacteriocidal immunity in the lung during *Mycobacterium bovis* BCG infection in C57BL/6 mice. *Infect. Immun.* 70: 5322–5327.

59. Francis, R. J., R. E. Butler, and G. R. Stewart. 2014. *Mycobacterium tuberculosis* ESAT-6 is a leukocidin causing Ca2+ influx, necrosis and neutrophil extracellular trap formation. *Cell Death Dis.* 5: e1474.
60. Weinberg, S. E., L. A. Sena, and N. S. Chandel. 2015. Mitochondria in the regulation of innate and adaptive immunity. *Immunity* 42: 406–417.
61. Segal, B. H., W. Han, J. J. Bushey, M. Joo, Z. Bhatti, J. Feminella, C. G. Dennis, R. R. Vethanayagam, F. E. Yull, M. Capitano, et al. 2010. NADPH oxidase limits innate immune responses in the lungs in mice. *PLoS One* 5: e9631.
62. Morgenstern, D. E., M. A. Gifford, L. L. Li, C. M. Doerschuk, and M. C. Dinauer. 1997. Absence of respiratory burst in X-linked chronic granulomatous disease mice leads to abnormalities in both host defense and inflammatory response to *Aspergillus fumigatus*. *J. Exp. Med.* 185: 207–218.
63. Schäppi, M., C. Deffert, L. Fiette, G. Gavazzi, F. Herrmann, D. Belli, and K. H. Krause. 2008. Branched fungal beta-glucan causes hyperinflammation and necrosis in phagocyte NADPH oxidase-deficient mice. *J. Pathol.* 214: 434–444.
64. van den Berg, J. M., E. van Koppen, A. Ahlin, B. H. Belohradsky, E. Bernatowska, L. Corbeel, T. Español, A. Fischer, M. Kurenko-Deptuch, R. Mouy, et al. 2009. Chronic granulomatous disease: the European experience. *PLoS One* 4: e5234.
65. de Luca, A., S. P. Smeekens, A. Casagrande, R. Iannitti, K. L. Conway, M. S. Gresnigt, J. Begun, T. S. Plantinga, L. A. Joosten, J. W. van der Meer, et al. 2014. IL-1 receptor blockade restores autophagy and reduces inflammation in chronic granulomatous disease in mice and in humans. *Proc. Natl. Acad. Sci. USA* 111: 3526–3531.
66. Meissner, F., K. Molawi, and A. Zychlinsky. 2008. Superoxide dismutase 1 regulates caspase-1 and endotoxic shock. *Nat. Immunol.* 9: 866–872.
67. Zhang, G., B. Zhou, S. Li, J. Yue, H. Yang, Y. Wen, S. Zhan, W. Wang, M. Liao, M. Zhang, et al. 2014. Allele-specific induction of IL-1β expression by C/EBPβ and PU.1 contributes to increased tuberculosis susceptibility. *PLoS Pathog.* 10: e1004426.
68. Marais, S., R. P. J. Lai, K. A. Wilkinson, G. Meintjes, A. O'Garra, and R. J. Wilkinson. 2017. Inflammasome activation underlying central nervous system deterioration in HIV-associated tuberculosis. *J. Infect. Dis.* 215: 677–686.
69. Tan, H. Y., Y. K. Yong, E. M. Shankar, G. Paukovics, R. Ellegård, M. Larsson, A. Kamarulzaman, M. A. French, and S. M. Crowe. 2016. Aberrant inflammasome activation characterizes tuberculosis-associated immune reconstitution inflammatory syndrome. *J. Immunol.* 196: 4052–4063.